Cardioprotective Effects of Rivaroxaban on Cardiac Remodeling After Experimental Myocardial Infarction in Mice

Nobuhiro Nakanishi, MD; Koichi Kaikita, MD, PhD; Masanobu Ishii, MD, PhD;
Yu Oimatsu, MD, PhD; Tatsuro Mitsuse, MD; Miwa Ito, MD, PhD;
Kenshi Yamanaga, MD, PhD; Koichiro Fujisue, MD, PhD; Hisanori Kanazawa, MD, PhD;
Daisuke Sueta, MD, PhD; Seiji Takashio, MD, PhD; Yuichiro Arima, MD, PhD;
Satoshi Araki, MD, PhD; Taishi Nakamura, MD, PhD; Kenji Sakamoto, MD, PhD;
Satoru Suzuki, MD, PhD; Eiichiro Yamamoto, MD, PhD;
Hirofumi Soejima, MD, PhD; Kenichi Tsujita, MD, PhD

Background: Direct-activated factor X (FXa) plays an important role in thrombosis and is also involved in inflammation via the protease-activated receptor (PAR)-1 and PAR-2 pathway. We hypothesized that rivaroxaban protects against cardiac remodeling after myocardial infarction (MI).

Methods and Results: MI was induced in wild-type mice by permanent ligation of the left anterior descending coronary artery. At day 1 after MI, mice were randomly assigned to the rivaroxaban and vehicle groups. Mice in the rivaroxaban group were provided with a regular chow diet plus rivaroxaban. We evaluated cardiac function by echocardiography, pathology, expression of mRNA and protein at day 7 after MI. Rivaroxaban significantly improved cardiac systolic function, decreased infarct size and cardiac mass compared with the vehicle. Rivaroxaban also downregulated the mRNA expression levels of tumor necrosis factor-α, transforming growth factor-β, PAR-1 and PAR-2 in the infarcted area, and both A-type and B-type natriuretic peptides in the non-infarcted area compared with the vehicle. Furthermore, rivaroxaban attenuated cardiomyocyte hypertrophy and the phosphorylation of extracellular signal-regulated kinase in the non-infarcted area compared with the vehicle.

Conclusions: Rivaroxaban protected against cardiac dysfunction in MI model mice. Reduction of PAR-1, PAR-2 and proinflammatory cytokines in the infarcted area may be involved in its cardioprotective effects.

Key Words: Cardiac remodeling; Myocardial infarction; Protease-activated receptor (PAR)-1; PAR-2; Rivaroxaban

Cardiac remodeling is an important prognostic factor in heart failure (HF).[1] Myocardial infarction (MI) is the most common cause of HF[2] and our understanding of the effect of cardiac remodeling in HF is based on MI studies.[3] The pathology of MI suggests that the inflammatory changes in the infarcted tissue correlate closely with cardiac function and prognosis after MI.[4,5] These findings suggest that modulation of the inflammatory response in the infarcted myocardium could potentially improve cardiac remodeling after MI.

Rivaroxaban, an oral anticoagulant, is used to prevent and treat atrial fibrillation and venous thrombosis, because it exerts its anticoagulant properties by inhibiting activated factor X (FXa).[6–10] It has been reported that combination therapies that include low-dose rivaroxaban seem to be effective in secondary prevention of acute coronary syndrome,[11] which suggests that rivaroxaban is effective not only for atrial fibrillation and venous thrombosis but also for coronary artery thrombosis. However, there is insufficient evidence about the cardioprotective effects of rivaroxaban on cardiac remodeling after MI.

Rivaroxaban also exhibits anti-inflammatory properties, acting through amelioration of protease-activated receptor (PAR)-1 and -2 in arteriosclerosis models.[12–17] In addition, basic in vivo and in vitro research work has examined in detail the relationship between PARs and cardiac remod-

Figure 1. Experimental protocol. CAL, coronary artery ligation; %FS, percent fractional shortening; UCG, ultrasound cardiography.
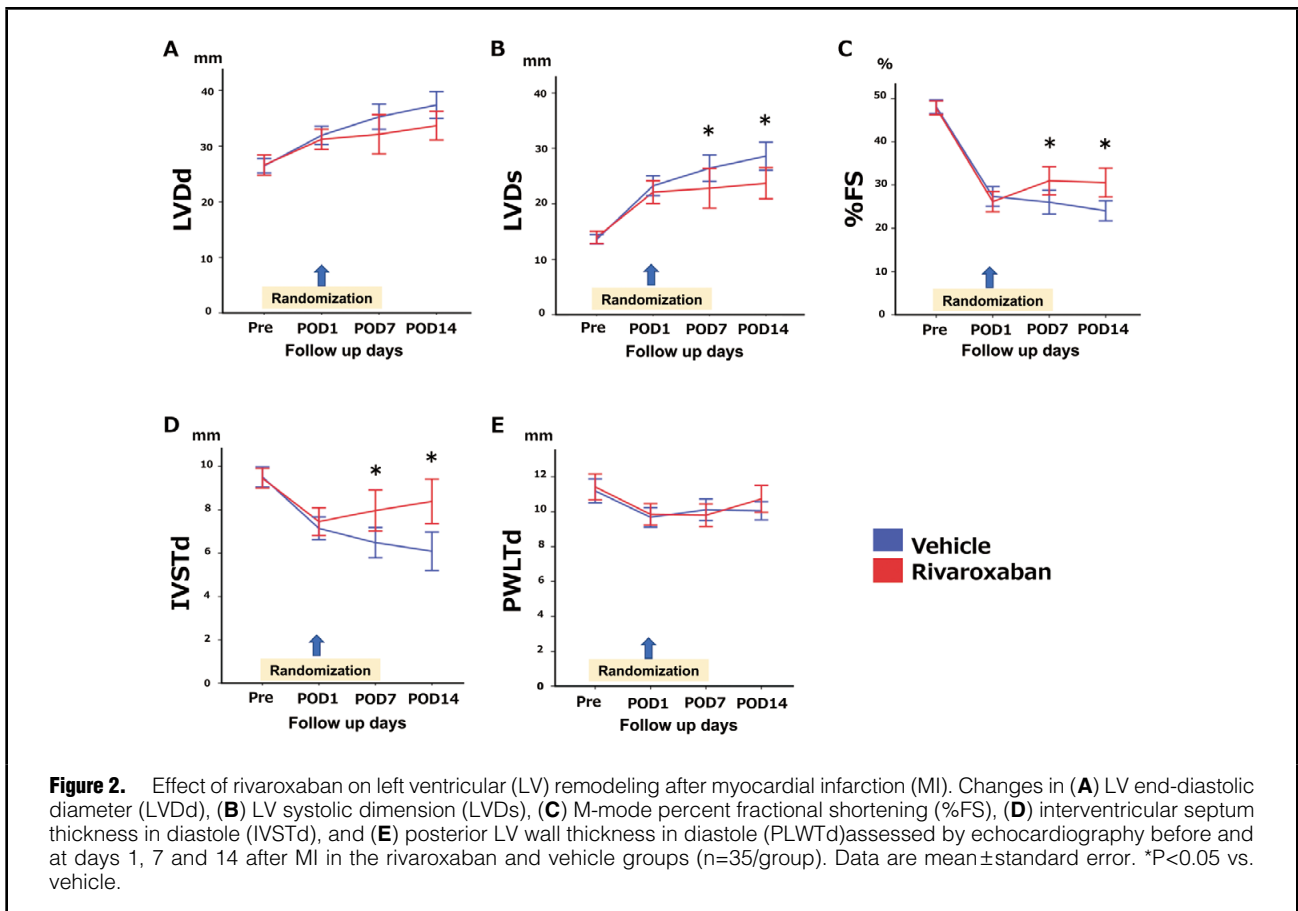
Figure 2. Effect of rivaroxaban on left ventricular (LV) remodeling after myocardial infarction (MI). Changes in (**A**) LV end-diastolic diameter (LVDd), (**B**) LV systolic dimension (LVDs), (**C**) M-mode percent fractional shortening (%FS), (**D**) interventricular septum thickness in diastole (IVSTd), and (**E**) posterior LV wall thickness in diastole (PLWTd) assessed by echocardiography before and at days 1, 7 and 14 after MI in the rivaroxaban and vehicle groups (n=35/group). Data are mean±standard error. *P<0.05 vs. vehicle.

eling.[18–21] Using wild-type (WT) and PAR-2-deficient mice, a recent experimental study showed that rivaroxaban suppressed cardiac remodeling after MI,[22] although the detailed underlying molecular mechanism of rivaroxaban was not demonstrated in the study.

Based on these observations, we hypothesized that rivaroxaban might contribute to cardiac remodeling after MI through the PAR-1 and PAR-2 pathways.

Methods

Animals
Male C57BL/6J (WT) mice were purchased from CLEA Japan Inc. (Tokyo, Japan). All mice were housed under a 12–12-h light–dark cycle and used for experiments between 9 and 12 weeks of age. Animal procedures were approved by the Animal Care and Use Committee of Kumamoto University, and conformed to the Guide for the Care and Use of Laboratory Animals published by the U.S. National Institutes of Health (publication No. 85-23, revised 1996).

Experimental Protocol
MI was induced by permanent ligation of the left anterior descending coronary artery at the level of the left atrium in anesthetized mice, as described in detail previously.[23] At day 1 after MI, echocardiography was performed as described in detail previously,[24] and the mice then were assigned at random to the rivaroxaban (kindly provided from Bayer
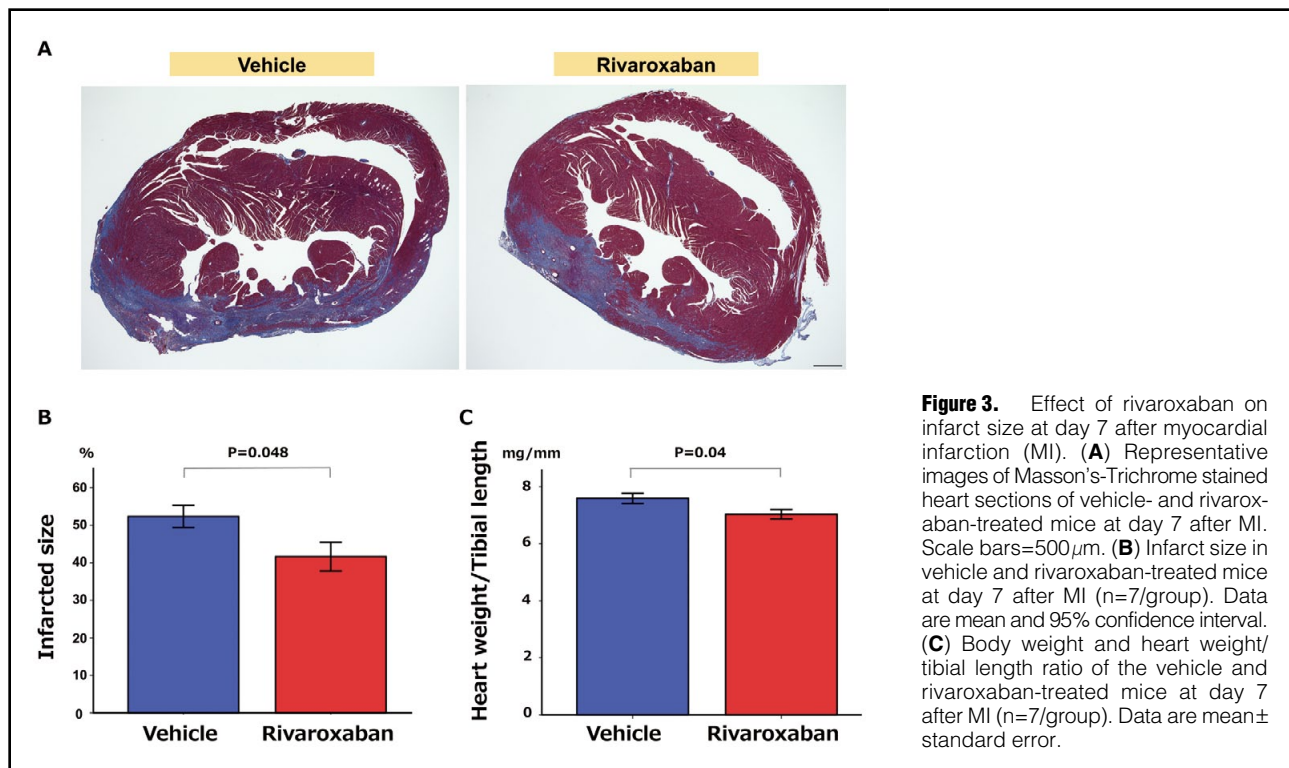
Figure 3. Effect of rivaroxaban on infarct size at day 7 after myocardial infarction (MI). (**A**) Representative images of Masson's-Trichrome stained heart sections of vehicle- and rivaroxaban-treated mice at day 7 after MI. Scale bars=500 μm. (**B**) Infarct size in vehicle and rivaroxaban-treated mice at day 7 after MI (n=7/group). Data are mean and 95% confidence interval. (**C**) Body weight and heart weight/tibial length ratio of the vehicle and rivaroxaban-treated mice at day 7 after MI (n=7/group). Data are mean± standard error.

HealthCare, Germany) or placebo group. All mice were provided with regular chow diet before randomization. After randomization, mice in the rivaroxaban group were provided with regular chow diet including rivaroxaban (2.4 g rivaroxaban/kg chow). The dietary dose of rivaroxaban in mice after MI was 138.5±50.3 mg/kg/day per mouse.

To determine the effect of treatment on cardiac function, echocardiography was repeated at day 7 and 14 after MI. Mice were anesthetized and the hearts were harvested for evaluation of mRNA and protein expression levels in the infarcted and non-infarcted regions by real-time reverse transcriptase-polymerase chain reaction (RT-PCR) assay and western blot analysis at day 7 after MI. Furthermore, we measured the infarct size and assessed the extent of inflammatory cell infiltration by histopathological analysis at day 7 after MI. The study protocol is shown in **Figure 1**.

Echocardiography Analysis
Each mouse was anesthetized with isoflurane and echocardiography was performed while the animal breathed spontaneously. We evaluated the M-mode percent fractional shortening (%FS), left ventricular (LV) diastolic dimension (LVDd), LV systolic dimension (LVDs), interventricular septum thickness in diastole (IVSTd), and posterior LV wall thickness in diastole (PLWTd) using the Xario system (Toshiba, Tokyo, Japan) with a 12-MHz linear array transducer.

Blood Sampling
It was assumed that rivaroxaban could potentially increase the likelihood of bleeding events. For this reason, we compared hemoglobin (Hb), hematocrit (Hct), mean corpuscular volume (MCV), and mean corpuscular Hb (MCH) between the rivaroxaban and placebo groups at day 14 after MI. Blood was collected from the right atrium into a tube containing EDTA-2Na (Terumo, Tokyo) and automatically analyzed using an ADVIA®2120i hematology system (Siemens Healthcare, Germany).

Histology and Immunohistochemistry
The harvested hearts were fixed in 4% paraformaldehyde, dehydrated, and embedded in paraffin. To determine the size of the MI-related scar, each sample at day 7 after MI was divided into 5 transverse sections from the apex to the base of the LV. The sections were stained with Masson trichrome to determine the size of the MI. The total circumference of the infarcted area was divided by the total LV circumference. Infarct length and total LV circumference were measured along the endocardial and epicardial surfaces in each section.[25] We analyzed cardiomyocyte cross-sectional area as described previously.[26] Immunohistochemistry was performed to determine the presence and type of inflammatory cells. Neutrophils and macrophages in the infarcted and non-infarcted areas were identified by staining with anti-Gr-1 (Southern Biotechnology, 1900-01) and anti-Iba1 (Wako Pure Chemical Industries, 019-19741), respectively. The number of positive cells was counted in 3 different fields. All measurements were performed with Image J software (National Institute of Health, Bethesda, MD, USA).

RT-PCR Assay
We evaluated the mRNA expression by RT-PCR, using the procedure described in detail previously.[27] Briefly, total RNA was extracted from the heart tissue at day 7 after MI using the RNA Easy Mini Kit (Qiagen, Hilden, Germany). The cDNA was synthesized using the T-PCR System 2700 (Applied Biosystems). RT-PCR was performed using a TaqMan Universal Master Mix kit with a CFX384 Real-Time System (Bio-Rad, Hercules, CA). We measured the
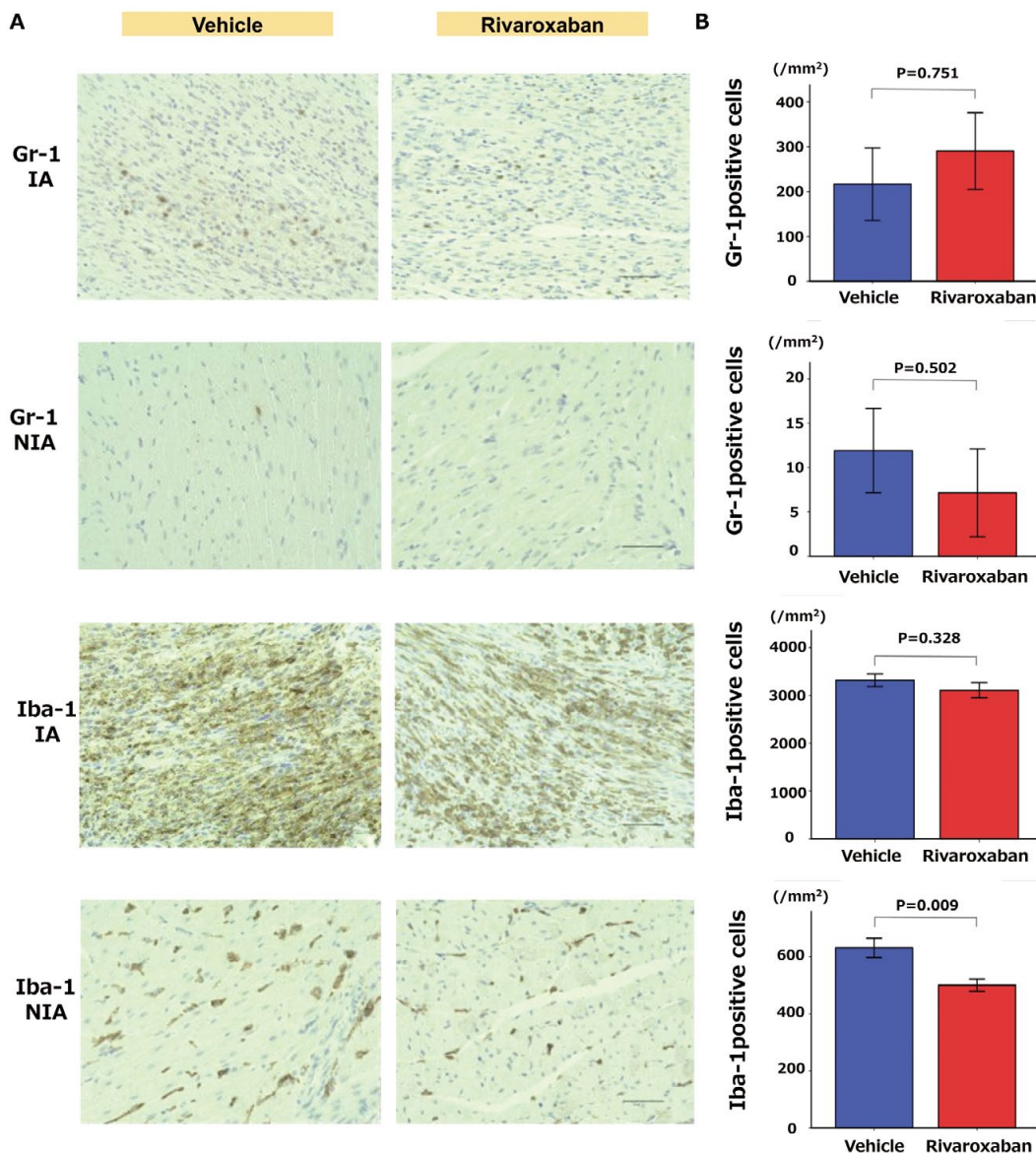
Figure 4. Characterization of inflammatory response at day 7 after myocardial infarction (MI). (**A**) Representative images of immunohistochemical staining with Gr-1 and Iba-1 of LV cross-sections in the vehicle- and rivaroxaban-treated mice at day 7 after MI. Scale bars=50μm (**B**) Density of Gr-1-positive macrophages and Iba-1-positive granulocytes in the infarcted area of the LV in vehicle- and rivaroxaban-treated mice at day 7 after MI. Data is mean±standard error (n=7/group). LV, left ventricle.

mRNA levels of A-type natriuretic peptide (ANP, GenBank Acc: NM_008725.3), B-type natriuretic peptide (BNP; NM_008726.5), collagen type 1 alpha1 (Col1α1; NM_007742.4), collagen type 3 alpha1 (Col3α1; NM_009930.2), interleukin-1 beta (IL-1β; NM_008361.4), interleukin-6 (IL-6; NM_031168.2), monocyte chemoat-tractant protein-1 (MCP-1; NM_011333.3), matrix metal-loproteinase-2 (MMP-2; NM_008610.2), MMP-9 (NM_013599.4), transforming growth factor-beta1 (TGF-β1; NM_011577.2), tissue inhibitor of metalloproteinase-1 (TIMP-1; NM_001044384.1), tumor necrosis factor-alpha (TNF-α; NM_013693.3), PAR-1 (NM_010169.3), PAR-2 (NM_007974.4), PAR-3 (NM_010170.4), and PAR-4 (NM_007975.4). The mRNA expression level was expressed relative to the expression level of the control (endogenous 18S ribosomal RNA gene).

Western Blot Analysis

Western blot analysis was performed with the SDS-PAGE Electrophoresis System, as described previously.[26] We used primary antibodies against phosohorylated extracellular signal-regulated kinase (p-ERK), ERK and glyceraldehyde-3-phosphate dehydrogenase (GAPDH) (Cell Signaling Technology, Danvers, MA, USA), in combination with a peroxidase-conjugated secondary antibody. The protein bands were detected with chemiluminescence. An ImageQuant LAS 4000 minibiomolecular imager (Fujifilm, Tokyo) was used for quantification of the band density.
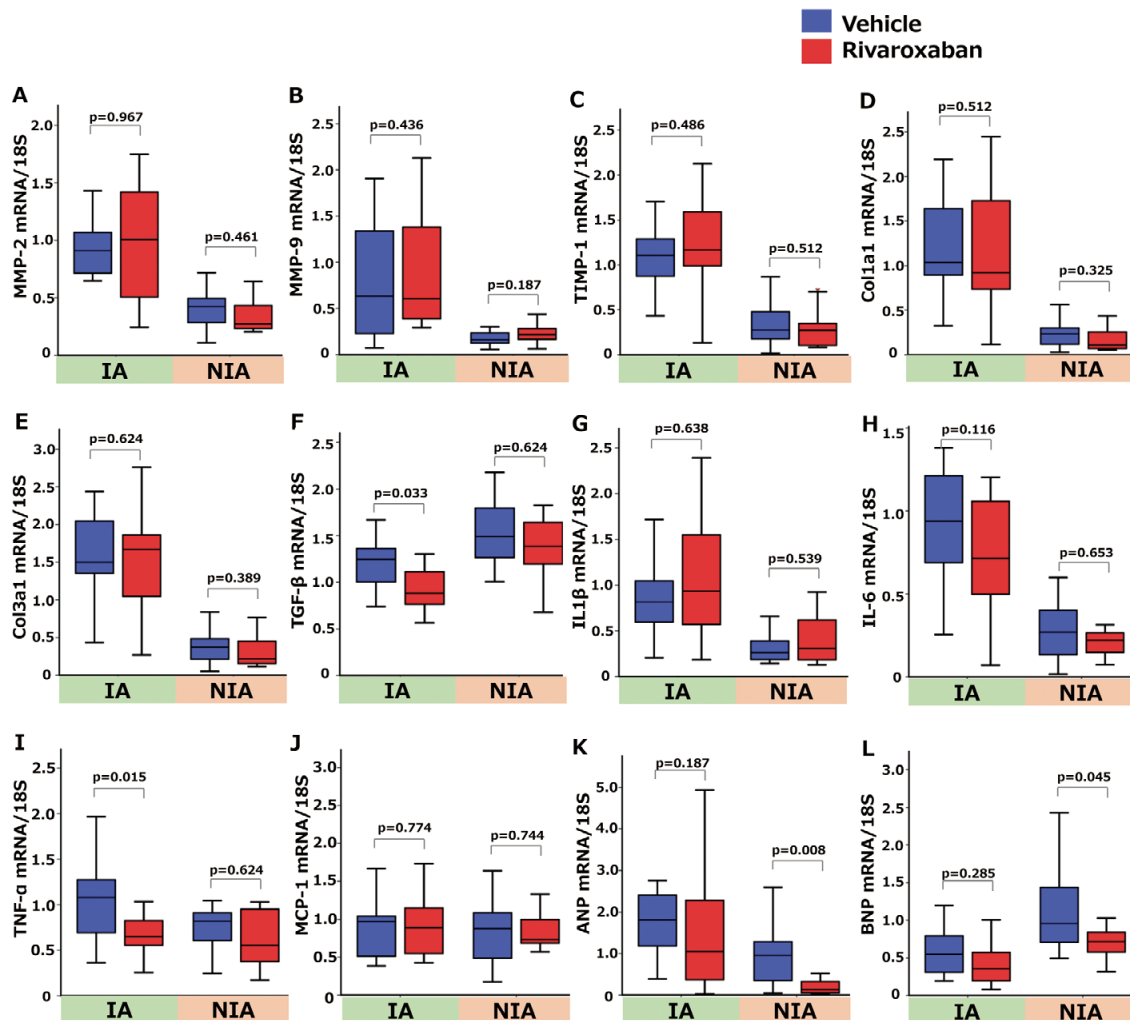
Figure 5. Effect of rivaroxaban on mRNA expression at day 7 after myocardial infarction (MI). Quantitative results of real-time reverse transcriptase PCR for (**A**) MMP-2, (**B**) MMP-9, (**C**) TIMP-1, (**D**) Col1a1, (**E**) Col3a1, (**F**) TGFb-1, (**G**) IL-1b, (**H**) IL-6, (**I**) TNF-α, (**J**) MCP-1, (**K**) ANP and (**L**) BNP mRNA levels at day 7 after MI. The mRNA level was expressed relative to the level of endogenous control 18S ribosomal RNA (n=15/group). In these box-and-whisker plots, lines within the boxes represent median values; the upper and lower lines of the boxes represent the 75th and 25th percentiles, respectively, and the upper and lower bars outside the boxes represent maximum and minimum values within 1.5-fold the interquartile range from the 75th and 25th percentile, respectively. ANP, atrial natriuretic peptide; BNP, brain natriuretic peptide; Col, collagen; IL, interleukin; IA, infarcted area; NIA, non-infarcted area; MCP, monocyte chemotactic protein; MMP, matrix metalloproteinase; PCR, polymerase chain reaction; TGF, tumor growth factor; TIMP, tissue inhibitor of metalloproteinase; TNF , tumor necrosis factor.
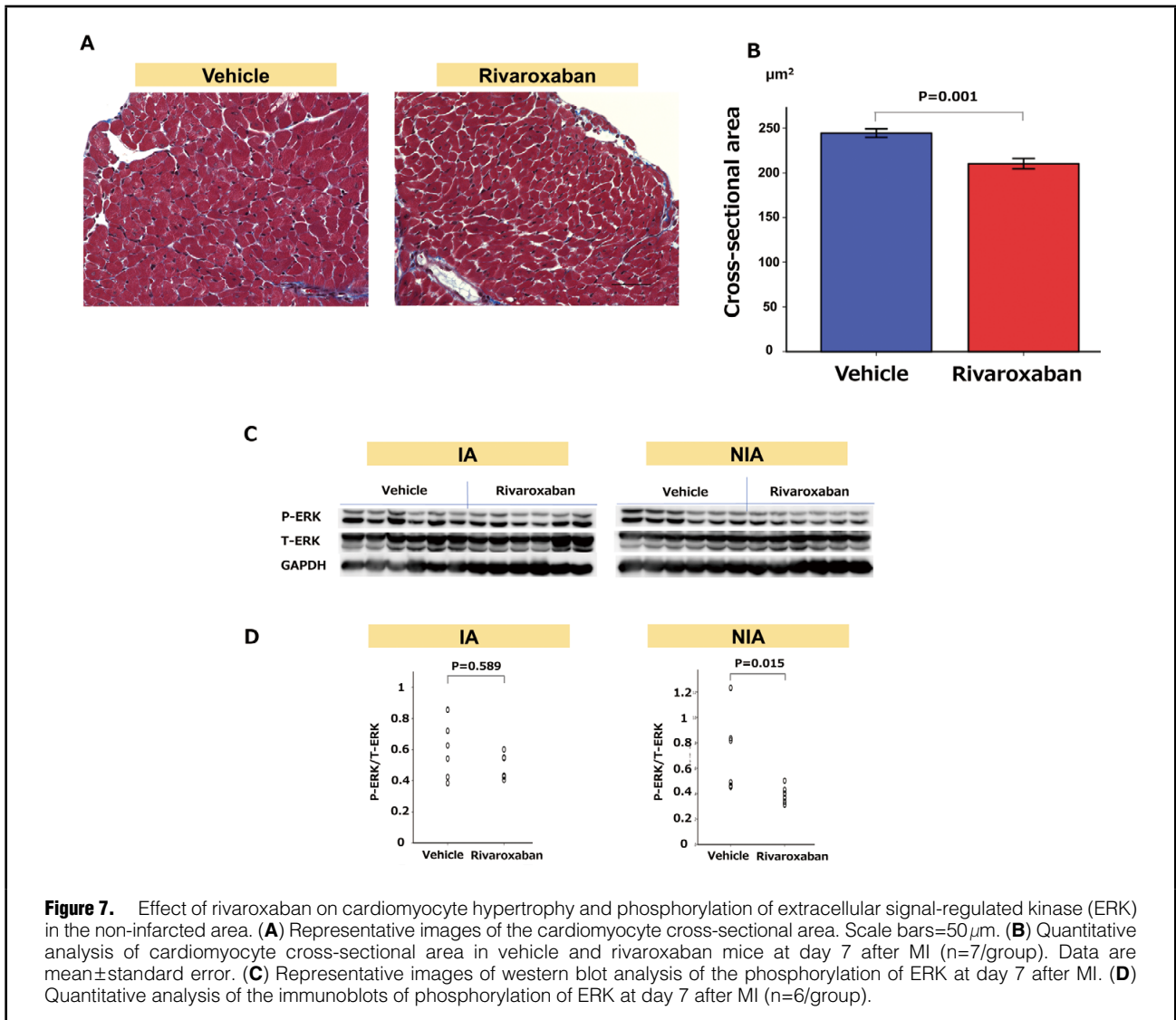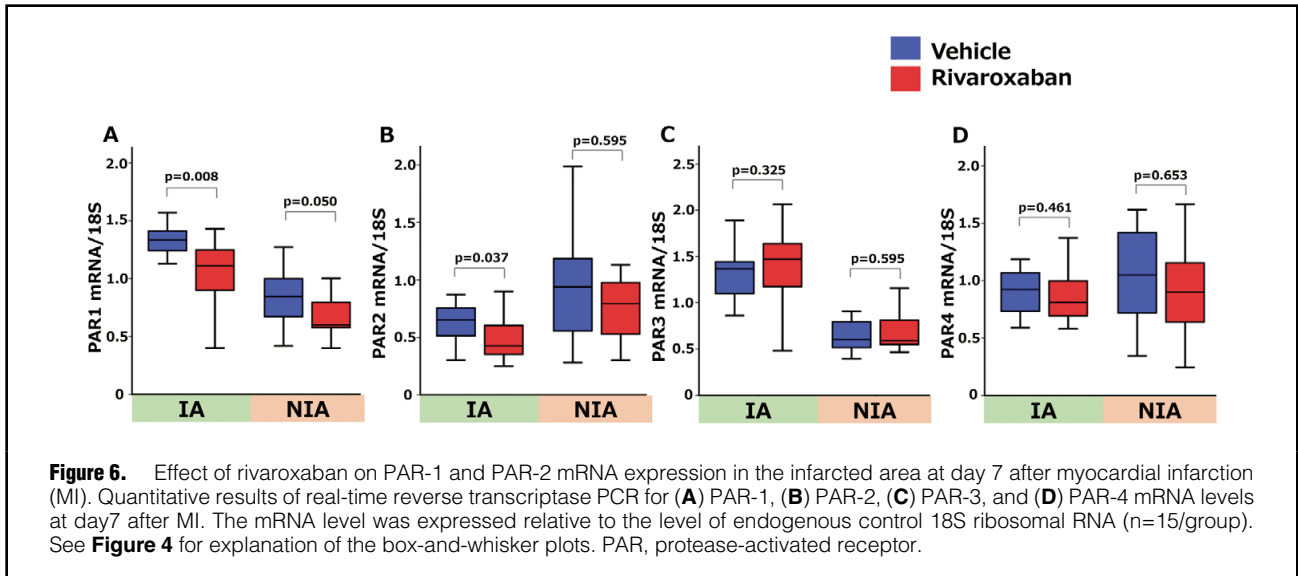
Statistical Analysis

Data of normally distributed continuous variables are expressed as mean±standard error, whereas those with skewed distribution are median (interquartile range). Differences between groups in infarct size, cardiac mass, number of inflammatory cells, cardiomyocyte cross-sectional area and parameters related to anemia were analyzed by unpaired Welch t-test. Differences in echo-cardiography variables were analyzed by the linear mixed model. Two-group comparisons of mRNA expression and density of protein were analyzed by the Mann-Whitney U test. A 2-tailed P-value of <0.05 was considered statistically significant. All statistical analyses were performed with the Statistical Package for Social Sciences software version 24.0 (IBM Corporation).

Results

Effects of Rivaroxaban on Echocardiographic Parameters and Bleeding Complications After MI

Figure 2 shows the echocardiographic parameters measured before MI and at day 1, 7 and 14 after MI. There were no significant differences between the 2 treatment groups in LVDd, LVDs, %FS, IVSTd, or PLWTd on the day before MI and the day after MI. However, LVDs, %FS, and IVSTd were significantly improved at day 7 and 14 after MI in the rivaroxaban group compared with the vehicle group, but there were no significant differences in LVDd and PLWTd between groups. In the analysis for serial changes in the echocardiographic parameters, 2 of 35 and 4 of 35 mice died in the vehicle and rivaroxaban groups,

Figure 6. Effect of rivaroxaban on PAR-1 and PAR-2 mRNA expression in the infarcted area at day 7 after myocardial infarction (MI). Quantitative results of real-time reverse transcriptase PCR for (**A**) PAR-1, (**B**) PAR-2, (**C**) PAR-3, and (**D**) PAR-4 mRNA levels at day7 after MI. The mRNA level was expressed relative to the level of endogenous control 18S ribosomal RNA (n=15/group). See **Figure 4** for explanation of the box-and-whisker plots. PAR, protease-activated receptor.

Figure 7. Effect of rivaroxaban on cardiomyocyte hypertrophy and phosphorylation of extracellular signal-regulated kinase (ERK) in the non-infarcted area. (**A**) Representative images of the cardiomyocyte cross-sectional area. Scale bars=50 μm. (**B**) Quantitative analysis of cardiomyocyte cross-sectional area in vehicle and rivaroxaban mice at day 7 after MI (n=7/group). Data are mean±standard error. (**C**) Representative images of western blot analysis of the phosphorylation of ERK at day 7 after MI. (**D**) Quantitative analysis of the immunoblots of phosphorylation of ERK at day 7 after MI (n=6/group).

respectively. The cause of death was cardiac rupture in all of the dead mice, which occurred 3–5 days after MI and the survival rate was identical between groups. Furthermore, there were no significant differences in Hb, Hct, MCV, or MCH at day 14 after MI (**Supplementary Figure**).

Histomorphometric and Immunohistochemical Analysis at Day 7 After MI

Because LVDs, %FS, and IVSTd improved significantly at day 7 after MI, we conducted histomorphometric analysis using samples obtained at day 7 after MI. As shown in **Figure 3A**, Masson's trichrome staining demonstrated myocardial fibrosis in the infarcted areas in both groups of mice; however, the infarct size was significantly smaller in the rivaroxaban group compared with the vehicle group (**Figure 3B**). Furthermore, rivaroxaban significantly attenuated heart weight/tibial length compared with the vehicle group at day 7 after MI (**Figure 3C**).

Figure 4A and **Figure 4B** show the results of immunohistochemical analysis at day 7 after MI. We calculated the density of Gr-1-positive granulocytes and Iba-1-positive macrophages in the infarcted and non-infarcted LV cross-sections of the vehicle- and rivaroxaban-treated mice at day 7 after MI. Rivaroxaban decreased the density of Iba-1-positive macrophages in the non-infarcted area compared with the vehicle, but did not affect the density of these cells in the infarcted area. There was no significant difference in the density of infiltrating Gr-1-positive granulocytes between groups.

Cardioprotective Effects of Rivaroxaban on Myocardial Gene Expression of Inflammatory Markers After MI

To investigate the mechanisms of rivaroxaban-induced improvement of cardiac function after MI, we evaluated the mRNA expression levels of cytokines involved in cardiac inflammation, tissue degradation, and fibrosis in the infarcted area at day 7 after MI. The mRNA expression levels of TNF-α and TGF-β in the infarcted area and those of ANP and BNP in the non-infarcted area were significantly lower in the rivaroxaban group compared with the vehicle group (TNF-α, P=0.015; TGF-β, P=0.033; ANP, P=0.008, BNP, P=0.045). On the other hand, the mRNA levels of MMP-2, MMP-9, TIMP-1, Col1a1, Col3a1, IL-1β, IL-6, and MCP-1 in the infarcted and non-infarcted area were almost identical between treatment groups (**Figure 5**).

As shown in **Figure 6**, PAR-1 and PAR-2 mRNA expression levels in the infarcted area, but not in the non-infarcted areas, were significantly lower in the rivaroxaban group compared with the vehicle group at day 7 after MI (PAR-1, P=0.008; PAR-2, P=0.037). Neither the pathological process of MI nor rivaroxaban had any effect on the mRNA expression levels of PAR-3 and PAR-4.

Effect of Rivaroxaban in the Non-Infarcted Myocardium

Because rivaroxaban improved cardiac dysfunction and reduced heart weight/tibial length compared with the vehicle group, we analyzed cardiomyocyte cross-sectional area in the myocardial sections at day 7 after MI. **Figure 7A** and **Figure 7B** show that rivaroxaban statistically attenuated cardiomyocyte hypertrophy in the non-infarcted area compared with the vehicle group at day 7 after MI.

To determine the molecular mechanisms of the cardioprotective effects of rivaroxaban, we performed western blot analysis for phosphorylation of ERK. The results demonstrated significant decreases in p-ERK in the non-infarcted

area (P=0.015), but not in the infarcted area at day 7 after MI in the rivaroxaban group compared with the vehicle group (**Figure 7C,D**).

Discussion

In this study, we showed that the cardiac remodeling process after MI improved with administration of rivaroxaban. Although it has been reported that rivaroxaban improves cardiac function through inhibition of PAR-2,[22] the exact underlying mechanism of such cardioprotective effects remains unknown. The present study extended previous observations of the cardioprotective effects of rivaroxaban after experimental MI by demonstrating that rivaroxaban protected against cardiac dysfunction in MI model mice probably by reducing the mRNA levels of PAR-1, PAR-2 and proinflammatory cytokines in the infarcted area.

PARs are a family of protease-mediated G protein-coupled 7 transmembrane receptors and so far 4 (PAR-1, PAR-2, PAR-3 and PAR-4) have been identified.[28–32] PAR-2 is activated by factor Xa, whereas PAR-1 is activated by not only factor Xa but also thrombin.[33] In this study, we found no significant differences in PAR-3 or PAR-4, compared with the vehicle, in the infarcted area at day 7 after MI; however, rivaroxaban significantly downregulated the mRNA expression of PAR-1, PAR-2, TNF-α and TGF-β. Using echocardiography, the present study demonstrated that rivaroxaban prevented excessive thinning of the IVSTd and improved cardiac function compared with the vehicle. In addition, pathological analysis demonstrated that rivaroxaban significantly reduced infarct size and heart weight. Previous studies using experimental MI models have demonstrated that inhibition of PAR-1 or PAR-2 downregulated the expression of proinflammatory cytokines and various markers of myocardial fibrosis.[18–22] Furthermore, in several experimental models of atherosclerosis, atrial fibrosis and ischemic cardiomyopathy, rivaroxaban also suppressed proinflammatory cytokines.[16–18,34] Based on these findings, it is conceivable that the cardioprotective effects of rivaroxaban are mediated through inhibition of PAR-1 and PAR2 in the infarcted area.

Various inflammatory reactions are associated with cardiac remodeling after MI.[35-42] Hara et al reported that stimulation of mice macrophages with FXa resulted in increases in inflammatory cytokines, and such increase was suppressed by rivaroxaban administration.[16] Other groups have demonstrated that rivaroxaban inhibits angiotensin II-induced functional activation in cultured cardiac fibroblasts,[43,44] and that rivaroxaban reduced the number of apoptotic cardiomyocytes and decreased the mRNA expression of proinflammatory cytokines.[34] In the present study, rivaroxaban interestingly reduced both TNF-α and TGF-β mRNA levels in the infarcted area.

Although TGF-β is known as a fibrotic factor,[45] it is also known as a modulator of proinflammatory cytokines, such as TNF-α.[46] In order to elucidate the role of TGF-β post-MI, further study will be needed to examine whether direct inhibition of TGF-β expression reflects the antifibrotic effect in the infarcted area after MI in rivaroxaban-treated and vehicle mice.

In the present study, there was no significant difference in the infiltration of inflammatory cells in the infarcted area between the rivaroxaban and vehicle groups, but rivaroxaban reduced the expression of proinflammatory cytokines in the infarcted area. Regarding this point, previous reports

have shown that stimulated macrophages, fibroblasts and cardiomyocytes express PAR-1 and PAR-2, and that rivaroxaban inhibited the activation of these cells through the suppression of PAR-1 and PAR-2.[16,34,43,44,47] It is possible that rivaroxaban could downregulate the activation of inflammatory cells and ischemic cardiomyocytes in the infarcted area by reducing the levels of PAR-1 and PAR-2, and then improve cardiac remodeling after MI, even though the numbers of inflammatory cells in the infarcted area were identical between the 2 treatment groups in the present study.

It is well known that MI leads to fibrosis and thinning in the infarcted area, which also induces compensated cardiac remodeling in the non-infarcted area and leads to cardiomyocyte hypertrophy of the non-infarcted area by overload pressure.[48] In the present study, rivaroxaban improved cardiac function and infarct size compared with the vehicle group. Analysis of cardiomyocyte cross-sectional area in the myocardial sections of the non-infarcted area showed that cardiomyocyte hypertrophy in response to MI was smaller in the rivaroxaban group than in the vehicle group. Furthermore, rivaroxaban reduced the mRNA expression levels of ANP and BNP mRNA expression levels and p-ERK in the non-infarcted area. Previous studies identified that increased ANP and BNP levels reflected cardiac overload in experimental MI models,[49] and that p-ERK is closely related to cardiac hypertrophy.[50,51] Based on these observations, it is possible that the cardioprotective effects of rivaroxaban through suppression of PAR-1, PAR-2 and proinflammatory cytokines in the infarcted area might prevent compensatory cardiomyocyte hypertrophy in the non-infarcted myocardium.

Study Limitations
First, the follow-up was limited to day 14 after MI, so the long-term effects of rivaroxaban on the myocardium after MI remain to be defined. Second, we did not analyze a PAR-1 and PAR-2 gain-of-function MI model. Previous reports demonstrated that PAR-1 overexpression induces eccentric hypertrophy and dilation.[19] In addition, PAR-2 overexpression also induces cardiac hypertrophy, fibrosis and inflammation.[20] Furthermore, myocardial ischemia–reperfusion leads to increased PAR-1 and PAR-2 expression, and both PAR-1 knockout mice and PAR-2 knockout mice had significant cardioprotective effects compared with WT mice in the same model.[19,21] Third, we did not perform in vitro studies to confirm the cardioprotective effects of rivaroxaban in the MI model. Regarding this point, previous studies using cultured and stimulated macrophages, fibroblasts and cardiomyocytes have already described the anti-inflammatory and antifibrotic effects of rivaroxaban.[16,34,43,44] We speculated that rivaroxaban might suppress the activation of these cells and regulate the inflammatory and fibrotic response in the infarcted lesions post-MI.

In conclusion, the present study showed that rivaroxaban protected against cardiac dysfunction in MI model mice. Rivaroxaban could be potentially beneficial for improvement of cardiac remodeling after MI.

IRB Information
The animal care and user committee of Kumamoto University granted an exemption from requiring ethics approval.

References
1. Cohn JN, Ferrari R, Sharpe N. Cardiac remodeling: Concepts and clinical implications: A consensus paper from an international forum on cardiac remodeling. Behalf of an International Forum on Cardiac Remodeling. *J Am Coll Cardiol* 2000; **35:** 569–582.
2. Lloyd-Jones D, Adams RJ, Brown TM, Carnethon M, Dai S, De Simone G, et al. Executive summary: Heart disease and stroke statistics – 2010 update: A report from the American Heart Association. *Circulation* 2010; **121:** 948–954.
3. Burchfield JS, Xie M, Hill JA. Pathological ventricular remodeling: Mechanisms. Part 1 of 2. *Circulation* 2013; **128:** 388–400.
4. Maekawa Y, Anzai T, Yoshikawa T, Sugano Y, Mahara K, Kohno T, et al. Effect of granulocyte-macrophage colony-stimulating factor inducer on left ventricular remodeling after acute myocardial infarction. *J Am Coll Cardiol* 2004; **44:** 1510–1520.
5. Frangogiannis NG. Regulation of the inflammatory response in cardiac repair. *Circ Res* 2012; **110:** 159–173.
6. Perzborn E, Strassburger J, Wilmen A, Pohlmann J, Roehrig S, Schlemmer KH, et al. In vitro and in vivo studies of the novel antithrombotic agent BAY 59-7939: An oral, direct Factor Xa inhibitor. *J Thromb Haemost* 2005; **3:** 514–521.
7. Roehrig S, Straub A, Pohlmann J, Lampe T, Pernerstorfer J, Schlemmer KH, et al. Discovery of the novel antithrombotic agent 5-chloro-N-({(5S)-2-oxo-3-[4-(3-oxomorpholin-4-yl) phenyl]-1,3-oxazolidin-5-yl}methyl)thiophene-2-carboxamide (BAY 59-7939): An oral, direct factor Xa inhibitor. *J Med Chem* 2005; **48:** 5900–5908.
8. Perzborn E, Roehrig S, Straub A, Kubitza D, Misselwitz F. The discovery and development of rivaroxaban, an oral, direct factor Xa inhibitor. *Nat Rev Drug Discov* 2011; **10:** 61–75.
9. Patel MR, Mahaffey KW, Garg J, Pan G, Singer DE, Hacke W, et al. Rivaroxaban versus warfarin in nonvalvular atrial fibrillation. *N Engl J Med* 2011; **365:** 883–891.
10. Bauersachs R, Berkowitz SD, Brenner B, Buller HR, Decousus H, Gallus AS, et al. Oral rivaroxaban for symptomatic venous thromboembolism. *N Engl J Med* 2010; **363:** 2499–2510.
11. Mega JL, Braunwald E, Wiviott SD, Bassand JP, Bhatt DL, Bode C, et al. Rivaroxaban in patients with a recent acute coronary syndrome. *N Engl J Med* 2012; **366:** 9–19.
12. Ishibashi Y, Matsui T, Ueda S, Fukami K, Yamagishi S. Advanced glycation end products potentiate citrated plasma-evoked oxidative and inflammatory reactions in endothelial cells by up-regulating protease-activated receptor-1 expression. *Cardiovasc Diabetol* 2014; **13:** 60.
13. Ishibashi Y, Matsui T, Fukami K, Ueda S, Okuda S, Yamagishi S. Rivaroxaban inhibits oxidative and inflammatory reactions in advanced glycation end product-exposed tubular cells by blocking thrombin/protease-activated receptor-2 system. *Thromb Res* 2015; **135:** 770–773.
14. Esmon CT. Targeting factor Xa and thrombin: Impact on

coagulation and beyond. *Thromb Haemost* 2014; **111:** 625–633.

15. Spronk HM, de Jong AM, Crijns HJ, Schotten U, Van Gelder IC, Ten Cate H. Pleiotropic effects of factor Xa and thrombin: What to expect from novel anticoagulants. *Cardiovasc Res* 2014; **101:** 344–351.

16. Hara T, Fukuda D, Tanaka K, Higashikuni Y, Hirata Y, Nishimoto S, et al. Rivaroxaban, a novel oral anticoagulant, attenuates atherosclerotic plaque progression and destabilization in ApoE-deficient mice. *Atherosclerosis* 2015; **242:** 639–646.

17. Hara T, Phuong PT, Fukuda D, Yamaguchi K, Murata C, Nishimoto S, et al. Protease-activated receptor-2 plays a critical role in vascular inflammation and atherosclerosis in apolipoprotein E-deficient mice. *Circulation* 2018; **138:** 1706–1719.

18. Kondo H, Abe I, Fukui A, Saito S, Miyoshi M, Aoki K, et al. Possible role of rivaroxaban in attenuating pressure-overload-induced atrial fibrosis and fibrillation. *J Cardiol* 2018; **71:** 310–319.

19. Pawlinski R, Tencati M, Hampton CR, Shishido T, Bullard TA, Casey LM, et al. Protease-activated receptor-1 contributes to cardiac remodeling and hypertrophy. *Circulation* 2007; **116:** 2298–2306.

20. Antoniak S, Sparkenbaugh EM, Tencati M, Rojas M, Mackman N, Pawlinski R. Protease activated receptor-2 contributes to heart failure. *PLoS One* 2013; **8:** e81733.

21. Antoniak S, Rojas M, Spring D, Bullard TA, Verrier ED, Blaxall BC, et al. Protease-activated receptor 2 deficiency reduces cardiac ischemia/reperfusion injury. *Arterioscler Thromb Vasc Biol* 2010; **30:** 2136–2142.

22. Bode MF, Auriemma AC, Grover SP, Hisada Y, Rennie A, Bode WD, et al. The factor Xa inhibitor rivaroxaban reduces cardiac dysfunction in a mouse model of myocardial infarction. *Thromb Res* 2018; **167:** 128–134.

23. Ishii M, Kaikita K, Sato K, Sueta D, Fujisue K, Arima Y, et al. Cardioprotective effects of LCZ696 (Sacubitril/Valsartan) after experimental acute myocardial infarction. *JACC Basic Transl Sci* 2017; **2:** 655–668.

24. Araki S, Izumiya Y, Rokutanda T, Ianni A, Hanatani S, Kimura Y, et al. Sirt7 contributes to myocardial tissue repair by maintaining transforming growth factor-beta signaling pathway. *Circulation* 2015; **132:** 1081–1093.

25. Matsusaka H, Ide T, Matsushima S, Ikeuchi M, Kubota T, Sunagawa K, et al. Targeted deletion of p53 prevents cardiac rupture after myocardial infarction in mice. *Cardiovasc Res* 2006; **70:** 457–465.

26. Fujisue K, Sugamura K, Kurokawa H, Matsubara J, Ishii M, Izumiya Y, et al. Colchicine improves survival, left ventricular remodeling, and chronic cardiac function after acute myocardial infarction. *Circ J* 2017; **81:** 1174–1182.

27. Araki S, Izumiya Y, Hanatani S, Rokutanda T, Usuku H, Akasaki Y, et al. Akt1-mediated skeletal muscle growth attenuates cardiac dysfunction and remodeling after experimental myocardial infarction. *Circ Heart Fail* 2012; **5:** 116–125.

28. Vu TK, Hung DT, Wheaton VI, Coughlin SR. Molecular cloning of a functional thrombin receptor reveals a novel proteolytic mechanism of receptor activation. *Cell* 1991; **64:** 1057–1068.

29. Nystedt S, Emilsson K, Wahlestedt C, Sundelin J. Molecular cloning of a potential proteinase activated receptor. *Proc Natl Acad Sci USA* 1994; **91:** 9208–9212.

30. Ishihara H, Connolly AJ, Zeng D, Kahn ML, Zheng YW, Timmons C, et al. Protease-activated receptor 3 is a second thrombin receptor in humans. *Nature* 1997; **386:** 502–506.

31. Xu WF, Andersen H, Whitmore TE, Presnell SR, Yee DP, Ching A, et al. Cloning and characterization of human protease-activated receptor 4. *Proc Natl Acad Sci USA* 1998; **95:** 6642–6646.

32. Kahn ML, Zheng YW, Huang W, Bigornia V, Zeng D, Moff S, et al. A dual thrombin receptor system for platelet activation. *Nature* 1998; **394:** 690–694.

33. Major CD, Santulli RJ, Derian CK, Andrade-Gordon P. Extracellular mediators in atherosclerosis and thrombosis: Lessons from thrombin receptor knockout mice. *Arterioscler Thromb Vasc Biol* 2003; **23:** 931–939.

34. Liu J, Nishida M, Inui H, Chang J, Zhu Y, Kanno K, et al. Rivaroxaban suppresses the progression of ischemic cardiomyopathy in a murine model of diet-induced myocardial infarction. *J Atheroscler Thromb* 2019; **26:** 915–930, doi:10.5551/jat.48405.

35. Horckmans M, Ring L, Duchene J, Santovito D, Schloss MJ, Drechsler H, et al. Neutrophils orchestrate post-myocardial infarction healing by polarizing macrophages towards a reparative phenotype. *Eur Heart J* 2017; **38:** 187–197.

36. Ma Y, Yabluchanskiy A, Lindsey ML. Neutrophil roles in left ventricular remodeling following myocardial infarction. *Fibrogenesis Tissue Repair* 2013; **6:** 11.

37. Nahrendorf M, Pittet MJ, Swirski FK. Monocytes: Protagonists of infarct inflammation and repair after myocardial infarction. *Circulation* 2010; **121:** 2437–2445.

38. Kaikita K, Hayasaki T, Okuma T, Kuziel WA, Ogawa H, Takeya M. Targeted deletion of CC chemokine receptor 2 attenuates left ventricular remodeling after experimental myocardial infarction. *Am J Pathol* 2004; **165:** 439–447.

39. Tsujita K, Kaikita K, Hayasaki T, Honda T, Kobayashi H, Sakashita N, et al. Targeted deletion of class A macrophage scavenger receptor increases the risk of cardiac rupture after experimental myocardial infarction. *Circulation* 2007; **115:** 1904–1911.

40. van Nieuwenhoven FA, Turner NA. The role of cardiac fibroblasts in the transition from inflammation to fibrosis following myocardial infarction. *Vascul Pharmacol* 2013; **58:** 182–188.

41. Talman V, Ruskoaho H. Cardiac fibrosis in myocardial infarction: From repair and remodeling to regeneration. *Cell Tissue Res* 2016; **365:** 563–581.

42. Nakaya M, Watari K, Tajima M, Nakaya T, Matsuda S, Ohara H, et al. Cardiac myofibroblast engulfment of dead cells facilitates recovery after myocardial infarction. *J Clin Invest* 2017; **127:** 383–401.

43. Kitasato L, Yamaoka-Tojo M, Hashikata T, Ishii S, Kameda R, Shimohama T, et al. Factor Xa in mouse fibroblasts may induce fibrosis more than thrombin. *Int Heart J* 2014; **55:** 357–361.

44. Hashikata T, Yamaoka-Tojo M, Namba S, Kitasato L, Kameda R, Murakami M, et al. Rivaroxaban inhibits angiotensin II-induced activation in cultured mouse cardiac fibroblasts through the modulation of NF-kappaB pathway. *Int Heart J* 2015; **56:** 544–550.

45. Border WA, Noble NA. Transforming growth factor beta in tissue fibrosis. *N Engl J Med* 1994; **331:** 1286–1292.

46. Lefer AM, Tsao P, Aoki N, Palladino MA Jr. Mediation of cardioprotection by transforming growth factor-beta. *Science* 1990; **249:** 61–64.

47. Antoniak S, Pawlinski R, Mackman N. Protease-activated receptors and myocardial infarction. *IUBMB Life* 2011; **63:** 383–389.

48. Pfeffer MA, Braunwald E. Ventricular remodeling after myocardial infarction: Experimental observations and clinical implications. *Circulation* 1990; **81:** 1161–1172.

49. Hama N, Itoh H, Shirakami G, Nakagawa O, Suga S, Ogawa Y, et al. Rapid ventricular induction of brain natriuretic peptide gene expression in experimental acute myocardial infarction. *Circulation* 1995; **92:** 1558–1564.

50. Molkentin JD, Dorn GW 2nd. Cytoplasmic signaling pathways that regulate cardiac hypertrophy. *Annu Rev Physiol* 2001; **63:** 391–426.

51. Takahashi N, Saito Y, Kuwahara K, Harada M, Kishimoto I, Ogawa Y, et al. Angiotensin II-induced ventricular hypertrophy and extracellular signal-regulated kinase activation are suppressed in mice overexpressing brain natriuretic peptide in circulation. *Hypertens Res* 2003; **26:** 847–853.

Supplementary Files